Special Issue: Unmanned Marine Systems

Regular Article

Path Following Using Rendezvous Dubins Curves and Integral Line-of-Sight for Unmanned Marine Systems

Brian R. Page, Reeve Lambert, Jalil Chavez-Galaviz and Nina Mahmoudian
School of Mechanical Engineering, Purdue University, West Lafayette, IN 47905

Abstract: Accurately following a prescribed path is critical for safe and efficient operation of autonomous systems in the field, especially for marine robots that typically operate away from human support and with sporadic communication abilities. Traditionally, variations of a lookahead control strategy have been employed for unmanned marine systems; however, these strategies can encounter problems when faced with disturbances and discontinuities in localization. In underwater applications, intermittent global localization updates are common due to constraints imposed by the lack of external updates from GPS. This paper examines the application of an online replanning tool based on Dubins curves to a path follower based on integral line-of-sight (ILOS) control. The fundamental idea is to drive the vehicle towards the prescribed path along a Dubins path. The proposed guidance strategy enables the path following controller to be tuned to aggressively track the path, improving disturbance rejection of an ILOS implementation without rendezvous ability by twofold in the simulated scenarios. The proposed method is experimentally validated on both an autonomous underwater vehicle and an autonomous surface vehicle with extended testing in a pond environment. Results indicate that the guidance strategy is able to track paths through disturbances and intermittent localization discontinuities in both surface and underwater use. This work has broad applications to field deployments of marine robots as a means to efficiently link mission level plans to vehicle level control signals considering realistic constraints on localization and control. Specific near-term applications focus on mobile underwater docking for undersea persistence.

Keywords: marine robotics, underwater robotics, guidance, navigation, control

1. Introduction

Deployment of autonomous vehicles in the marine environment is characterized by large disturbances and potentially poor localization information being updated at erratic intervals (Leonard and Bahr, 2016). Despite these challenges, long-term field operation is critical for a wide range of marine science and surveillance missions (Li et al., 2018, 2019). These missions often result in vehicles operating far

Received: 15 February 2021; revised: 10 February 2022; accepted: 31 July 2022; published: 21 September 2022.

Correspondence: Nina Mahmoudian, School of Mechanical Engineering, Purdue University, West Lafayette, IN 47905, Email: ninam@purdue.edu

DOI: https://doi.org/10.55417/fr.2022060

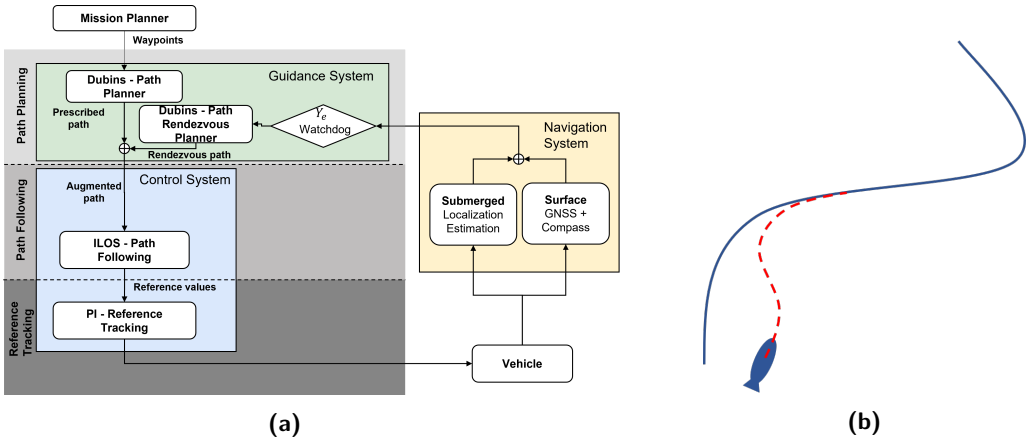

Figure 1. (a) Multilayer Guidance and Navigational Control (GNC) Architecture: at the path planning layer is the Dubins path planner which generates the prescribed path. At the same layer is the path rendezvous planner, which injects rendezvous paths when required to return to the prescribed path. The integral line-of-sight controller at the path following layer calculates reference headings based on the augmented path. The reference tracking layer creates actionable rudder commands to navigate the vehicle along the path. (b) Sketch of the guidance strategy: the prescribed path is blue; the rendezvous path is in red dashed lines.

from human operators in open water and require a high degree of autonomy to adapt to changing conditions.

One common theme across the range of marine robots is the overall guidance strategy (Figure 1a). In the standard navigation approach, there are three layers consisting of a path planning layer, a path following layer, and a reference tracking layer (Bychkov et al., 2019; Carreras et al., 2018; Ridao et al., 2000). Each of these layers contributes significantly towards overall operational efficiency of the vehicle.

At the path planning layer is the Dubins path planner, which receives a list of waypoints from the mission planner. The latter is sometimes a human operator or an intelligent tool (Li et al., 2018). The goal of the layer is to design paths for the vehicle to follow to achieve the mission such as seafloor mapping. Depending on the mission, a full 3D path may be developed (Zhou et al., 2019) or a more rudimentary list of waypoints may be used such as in lawnmower paths (Li et al., 2019). In either case, the goal is almost always to follow a minimum time curve. The output of the path planning layer is a prescribed path for the Autonomous Underwater Vehicle (AUV) to follow, and achieve the desired mission.

In the path following layer, the controller attempts to drive the vehicle to track the prescribed path. This is typically challenged by time-varying disturbances (Li et al., 2019) as well as poor localization information while submerged that may result in discontinuities in position estimation when at the surface or in acoustic communication range (Rypkema et al., 2017). A wide assortment of path following controllers exists; however, most revolve around some form of a lookahead or line-of-sight controller (Caharija et al., 2012; Fossen and Lekkas, 2017). These controllers are generally capable of handling some disturbances and tracking with reasonable accuracy, but are limited due to the inherent trade-off between disturbance rejection and stability through discontinuities.

At the reference tracking layer is the vehicle-specific reference tracking controller such as a heading controller on an Autonomous Surface Vehicle (ASV). Reference tracking is generally a platform-specific problem and is not considered for this paper. Outside of this structure is the localization stack onboard the vehicle which is platform and domain specific. The localization problem is challenging, particularly in the underwater environment, and is not considered as part of this work.

This paper examines augmenting the classic integral line-of-sight (ILOS) control strategy with a novel Dubins path rendezvous planner at the path planning layer that generates an efficient

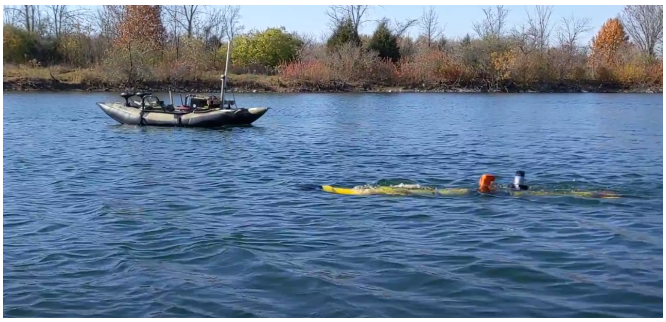

Figure 2. Experimental platforms used in this paper: a custom autonomous surface vehicle with differential steering and an Oceanserver Iver3 autonomous underwater vehicle.

rendezvous path when disturbed from the prescribed path. The fundamental idea of the Dubins path rendezvous planner is to update the prescribed path with time optimal rendezvous curves whenever a sufficiently large deviation from the prescribed path is detected (Manyam and Rathinam, 2018; Techy and Woolsey, 2009; Techy et al., 2010). The Dubins path rendezvous planner is a planar curve rapidly calculated online by approximating the vehicle as a car that can travel at a constant speed with turns up to a maximum rate (Mahmoudian et al., 2010; Tinka et al., 2009). Due to this approximation, the optimal rendezvous will always consist of a series of turn-straight-turn or turn-turn-turn, the so-called Dubins set (Dubins, 1957). With this augmented path, the ILOS path following controller will never need to track a path through large disturbances such as discontinuities in localization. This enables the ILOS path following controller to be tuned much more aggressively than normally allowable for stability. The new path following controller is then able to accurately track the augmented path with greater disturbance rejection. This strategy enables rapid experimental adaptation to any vehicle that can be approximated as a Dubins car across domains such as surface and underwater vehicles. The proposed method is evaluated on a variety of scenarios with an underwater vehicle simulation as well as extensively experimentally validated on an Oceanserver Iver3 AUV and custom ASV (Figure 2). In total, 30 hours of experimental underwater operation and 5 hours of surface operation are presented here.

The remainder of this paper will discuss background in Section 2, guidance strategy design in Section 3, simulation setup and results in Section 4, field setup and results in Section 5, and a brief conclusion in Section 6. The goal is to present the method, setup, and results to prove the effectiveness of the proposed approach for applications in both the underwater and surface domains on a variety of missions.

2. Background

2.1. Path Planning

Path planning for marine systems can generally be considered to operate on two disparate scales. On the large scale, overall mission planners are capable of generating plans for a fleet of vehicles to perform area coverage missions based either on the standard lawnmower path (Li et al., 2019) or more complex routings (Li et al., 2018). On the smaller scale, path planners generate curvilinear paths for the vehicle to follow versus simple waypoint routings. This strategy has evolved with complex three-dimensional paths being generated for specific missions such as shipwreck mapping (Viswanathan et al., 2017) and iceberg studies (Zhou et al., 2019). For waypoint-based missions, the discrete waypoints are generally interpreted into straight linear paths for the path following algorithm onboard the vehicle to track. Another option is to connect the waypoints using time optimal curves, also known as Dubins curves. These curves are the minimum time control policy to drive from one point and heading to another point and heading (Dubins, 1957) and always consist of a series of turn-straight-turn or turn-turn-turn (Figure 3). A brief discussion of Dubins paths is

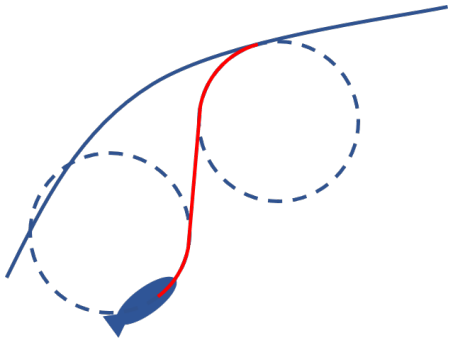

Figure 3. Dubins path planning to generate rendezvous path. The prescribed path is the solid blue path. The vehicle actually starts away from the path. The dashed lines represent the turn radius and the red path is the true path followed. The point where the rendezvous path returns to the prescribed path is called the rendezvous distance, δ.

included below for completeness, with a detailed description of the rapid calculation process included in Shkel and Lumelsky (2001).

Consider the path between an initial location and final location, each with a prescribed heading angle. These are called the initial (P_i, α) and final (P_f, β) configurations that define two points in the configuration space and define boundary conditions. The goal is to calculate a minimum distance smooth path between these configurations with curvature limited by $1/\rho$ when ρ is the turn radius. This problem was first solved by Dubins (1957). The solution is called the Dubins set, $\mathcal{D}$, and consists of $\mathcal{D} = \{LSL, RSR, RSL, LSR, RLR, LRL\}$ where L is a left turn at maximum rate, R is a right turn at maximum rate, and S is a straight segment with no turning. The Dubins set has been validated many times with different calculation approaches (Boissonnat et al., 1994; Reeds and Shepp, 1990). For the purposes of this paper, we follow the approach in Shkel and Lumelsky (2001). This strategy enables efficient calculation of the shortest path in the configuration space through the creation of equivalency groups based on angle quadrants of the starting and ending configurations.

To calculate the shortest path between starting and ending configurations, we first define admissible paths as a concatenation of the three elementary motions (left, right, straight):

$$\begin{aligned} L_v(x,y,\phi) &= (x + \sin(\phi+v) - \sin(\phi), \\ &\quad y - \cos(\phi+v) + \cos(\phi), \phi + v) \\ R_v(x,y,\phi) &= (x - \sin(\phi-v) + \sin(\phi), \\ &\quad y + \cos(\phi-v) - \cos(\phi), \phi - v) \\ S_v(x,y,\phi) &= (x + v\cos(\phi), y + v\sin(\phi), \phi), \end{aligned} \tag{1}$$

where (x, y, ϕ) is the vehicle position and heading, and v is segment length. Using these elementary transformations, we can define any path in the Dubins set. For example, a RSL path with respective segment lengths of t, p, q is defined as $R_q(S_p(L_t(x, y, \phi)))$ with total path length $\mathcal{L} = t + p + q$.

Calculation of path lengths for each admissible path in the Dubins set is computationally expensive, so in Shkel and Lumelsky (2001) the problem is transformed into a set of equivalency groups based on the requirement that each path in the Dubins set always begins and ends with a curve. This enables the problem to be simplified significantly based on angular quadrants of the initial and final headings and switching functions defined for each case (Table 1). Specific switching functions for each case along with a detailed derivation are available in Shkel and Lumelsky (2001).

2.2. Path Following

Navigation of marine vehicles along a prescribed path has been completed using a variety of methods; however, one common approach is to utilize variations on the lookahead control strategy (Coulter,

Table 1. Dubins path decision table for long path case ($d > 4\rho$) (Shkel and Lumelsky, 2001).

Initial \ Final	1	2	3	4
1	RSL	if $S_{12} < 0$ then RSR else RSL	if $S_{13} < 0$ then RSR else LSR	if $S_{14}^1 > 0$ then LSR if $S_{14}^2 > 0$ then RSL else RSR
2	if $S_{21} < 0$ then LSL else RSL	if $S_{22}^1 < 0$ then LSL if $S_{22}^1 > 0$ then RSL if $S_{22}^2 < 0$ then RSR if $S_{22}^2 > 0$ then RSL	RSR	if $S_{24} < 0$ then RSR else RSL
3	if $S_{31} < 0$ then LSL else LSR	LSL	if $S_{33}^1 < 0$ then RSR if $S_{33}^1 > 0$ then LSR if $S_{33}^2 < 0$ then LSL if $S_{33}^2 > 0$ then LSR	if $S_{34} < 0$ then RSR else LSR
4	if $S_{41}^1 > 0$ then RSL if $S_{41}^2 > 0$ then LSR else LSL	if $S_{42} < 0$ then LSL else RSL	if $S_{43} < 0$ then LSL else LSR	LSR

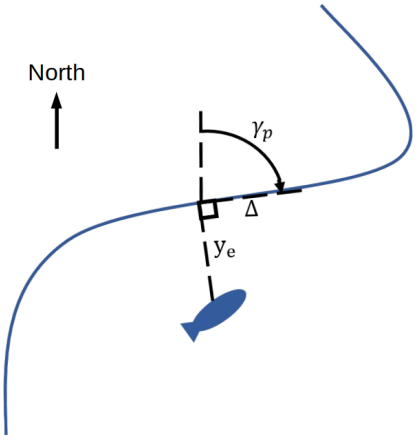

Figure 4. Line-of-sight controller parameters. y_e is cross-track error, Δ is lookahead distance, γ_p is projected heading.

1992; Fossen and Lekkas, 2017), especially when considering fixed depth operations. In this strategy, the vehicle's position is projected onto the path, a point directly ahead along the path vector is selected, and then the vehicle drives towards that point with a hybrid of pursuit towards the lookahead point and pursuit directly towards the path. This control style is experimentally extremely robust and has seen widespread use in industry across domains (Kim et al., 2007; Oh and Sun, 2010). One specific implementation of this control strategy is integral line-of-sight guidance (Borhaug et al., 2008; Caharija et al., 2016; Fossen and Lekkas, 2017; Fossen et al., 2015). In this control strategy the vehicle is required to converge to a path in the presence of environmental disturbances (Figure 4). The guidance law is defined as follows:

$$\phi_D = \gamma_p + \tan^{-1}\left(-\frac{1}{\Delta}y_e - \hat{\beta}\right) \tag{2}$$

where ϕ_D is the desired heading, γ_p is the projected heading which is the prescribed heading of the path at the point on the path being tracked when measured from due north (0 degrees), Δ is the lookahead distance, y_e is cross-track error, and $\hat{\beta}$ is the estimate of sideslip angle based on the integral of Equation (3). Lookahead distance (Δ) is user selected and can be based on an adaptive

controller with the input $\Delta\hat{\beta}$ subject to $0 < \Delta_{min} \leq \Delta \leq \Delta_{max}$:

$$\dot{\hat{\beta}} = \gamma \frac{U\Delta}{\sqrt{\Delta^2 + \left(y_e + \Delta\hat{\beta}\right)^2}} y_e, \gamma > 0 \tag{3}$$

where U is vehicle forward velocity and γ is adaptation gain.

Validation of line-of-sight control strategies in literature are typically completed on the maneuvering models from Fossen (1994) with papers exploring applications to different vehicles and varying levels of realism. Such line-of-sight control strategies have been shown to be accurate for long duration missions and can be combined with terminal homing approaches to enable a unified underwater docking strategy (Page and Mahmoudian, 2020; Page et al., 2021).

The contribution of this work lies at the junction of controller design, path planning, and path following. Overall mission design and vehicle-specific reference tracking are outside the scope of this work but the proposed approach links the two in a generalizable manner across missions, platforms, and domains.

3. Guidance Strategy

This paper presents the idea of generating local Dubins paths to rendezvous with the prescribed path from the path planning layer. Fundamentally, this can be thought of as adding an additional control block at the path planning layer between the Dubins path planner and the ILOS path following controller, creating a multi-layer guidance strategy for the AUV (Figure 1a). Each control layer operates asynchronously, generating reference outputs for the lower layers to operate on. Unlike other control strategies such as the supervisory controller (Battistelli et al., 2012, 2013; Torrico et al., 2016; Xu et al., 2004), the proposed approach does not switch gains from a given set of candidate controllers; instead, it provides an augmented path to the path following layer that enables a more aggressive tuning at the path following layer for the unique reference tracking controller of the system. Combined, this results in an overall navigational controller.

At the path planning layer is the Dubins path planner that generates the prescribed path. For the purposes of this paper we assume that the waypoints and paths are known a priori and a prescribed path joining these points is defined as an ordered series of points spaced 1 m apart on the path. At the same layer a Dubins path rendezvous planner can inject augmented paths if large cross-track errors are detected. The ILOS path following then takes the augmented path and creates reference headings which are acted on by the proportional-integral (PI) reference tracking controller.

At the Dubins path rendezvous planner, we take the vehicle's current position and find its nearest point on the prescribed path. If the prescribed path is far away, we augment the path with an additional rendezvous Dubins path that originates at the vehicle's current realized position and terminates at a location on the prescribed path that is some rendezvous distance (δ) ahead of the point on the prescribed path the vehicle is tracking (Figure 1b). The vehicle then begins to follow the path comprised of the rendezvous path joined with the prescribed path beyond the point of rendezvous. The rendezvous path is only generated whenever a sufficiently large error from the prescribed path (or earlier rendezvous path) exists. If, after affixing to the rendezvous path, the cross-track error y_e increases again to a level requiring a further replan, a new rendezvous path is created back to the prescribed path and the previous rendezvous path is discarded. This limits computational load to just barely higher than a stand-alone path following controller. In practice, the rendezvous path will only be generated when very large disturbances or updates in location estimate occur, such as those that occur when surfacing for global navigation satellite system (GNSS) access.

In real-world applications the rate of rendezvous path creation is related to the frequency of GNSS acquisition (surfacing) and the magnitude and direction of time varying disturbances. The minimum time between rendezvous path generations is bounded by the time it takes the vehicle to travel far enough from the path to accumulate enough cross-track error to warrant the generation of another rendezvous path. In the event of GPS localization noise greater than the replan threshold

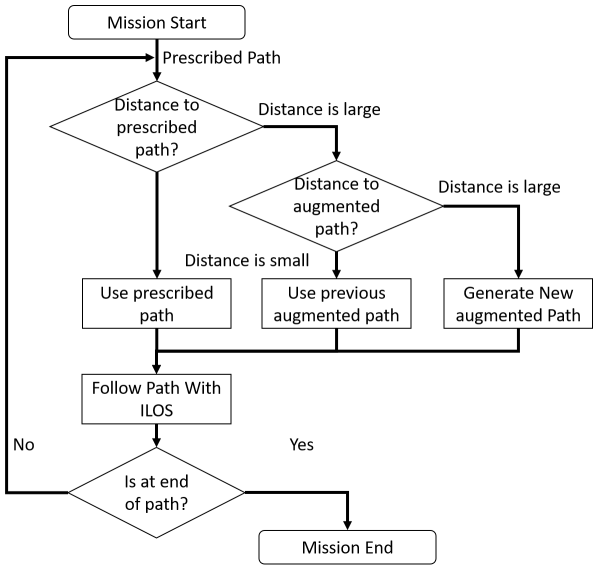

Figure 5. Integral line-of-sight (ILOS) control with 2D Dubins replanning algorithm.

issues can arise. Furthermore, input saturation is not explicitly addressed for this system. The proposed method addresses potential input saturation by setting the planned turn radius (ρ) of the Dubins curves to be slightly larger than the minimum turn radius achievable by the vehicle. This ensures that the planned paths are feasible to be tracked while rejecting minor disturbances. If disturbances are too great during path following operations, the cross-track error will slowly grow until a rendezvous path is generated originating at the vehicle's position.

The path following layer tracks the augmented path or prescribed path as controlled by the Dubins path rendezvous planner until the mission is completed. For this paper, an ILOS controller was used, but any variety of path following algorithm can be applied with the path rendezvous control strategy.

The algorithm is outlined in flowchart format in Figure 5. With the addition of the rendezvous Dubins paths, we can guarantee that the path following controller will never need to follow a path that is far from the current vehicle location. This enables the ILOS path following controller to be tuned very aggressively for better disturbance rejection. The Dubins path rendezvous planner adds one more tunable parameter which is the rendezvous distance (δ). Selection of this parameter is currently manual, but may be optimized in the future or made adaptive.

As an example scenario, assume that the vehicle is located away from the path in Figure 3. The prescribed path is the blue line. The cross-track error is above the threshold which triggers the Dubins path rendezvous planner to create a new Dubins path from the current location to a point on the prescribed path at distance δ ahead.

In any scenario, if the cross-track error is large enough to trigger the generation of a new rendezvous path, the prior rendezvous path is first discarded, and then the new rendezvous path is planned back to the prescribed path. The ILOS controller then attempts to follow this augmented path.

At the reference tracking layer, the reference heading is interpreted by a vehicle-specific controller. For the underwater vehicles, we control thrust, depth, and heading as independent parameters. Low level control of thrust uses a classic proportional-integral-derivative (PID) controller to track a reference velocity. Control of depth is achieved with a nested depth/pitch PID control loop described in Page and Mahmoudian (2019). Control of vehicle heading is achieved with a PID heading controller acting on the rudder. On the surface vehicle, we control overall thrust and turn rate.

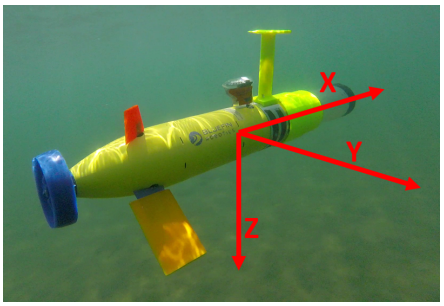

Figure 6. The Bluefin SandShark is a 1.2-m-long AUV capable of performing moderate endurance missions. The body-fixed frame (red) is located at the center of buoyancy of the AUV, the earth-fixed frame is located at an arbitrary location in the water, and the flow frame travels with the current.

4. Underwater Simulation

4.1. Simulation Setup

The guidance strategy proposed in this paper was simulated using a full six-degree-of-freedom hydrodynamic simulation of an AUV. This is compared to the more typical reduced order models used for path following algorithm validation. The additional computational complexity enables this work to be extended to more complex missions beyond path following as well as aids in the transition to field experiments. The dynamic model used in this paper is based on prior work (Page and Mahmoudian, 2020; Zhang et al., 2017). Consistent with this work, some assumptions are required to model the vehicle dynamic system:

- The AUV is trimmed perfectly neutral with a small purely vertical distance between center of mass and center of buoyancy to self-right the vehicle.
- The thruster is assumed to be a purely forward force.
- Environmental disturbances are modeled by the flow frame which adds to the vehicle velocity for the calculation of hydrodynamic terms.

In accordance with Fossen (1994), three frames are used and defined in Figure 6. The relative movement of the body-fixed frame relative to the flow frame is used to calculate forces and moments applied to the vehicle as the summation of the vehicle's viscous and inviscid hydrodynamic terms. The viscous forces (f_v) and moments (m_v) are expressed as follows:

$$\begin{aligned} \boldsymbol{f}_v &= \begin{pmatrix} X_v \\ Y_v \\ Z_v \end{pmatrix}, \\ \boldsymbol{m}_v &= \begin{pmatrix} K_v \\ M_v \\ N_v \end{pmatrix}. \end{aligned} \tag{4}$$

The forces and moments are nondimensionalized with $0.5\rho V^2 L^2$ and $0.5\rho V^2 L^3$, where V is the magnitude of velocity and L is the characteristic length.

$$\begin{aligned} X'_v &= \frac{X_v}{0.5\rho V^2 L^2}, \quad Y'_v = \frac{Y_v}{0.5\rho V^2 L^2}, \quad Z'_v = \frac{Z_v}{0.5\rho V^2 L^2}, \\ K'_v &= \frac{K_v}{0.5\rho V^2 L^3}, \quad M'_v = \frac{M_v}{0.5\rho V^2 L^3}, \quad N'_v = \frac{N_v}{0.5\rho V^2 L^3}. \end{aligned} \tag{5}$$

Following Nelson (1998) and Pamadi (2004), the nondimensional quantities are calculated in Equations (6). In these equations α and β are angle of attack and sideslip angles, δ_r and δ_e are

rudder and elevator angles, and angular velocities are the nondimensional $\bar{p} = \frac{pL}{V}$, $\bar{q} = \frac{qL}{V}$, and $\bar{r} = \frac{rL}{V}$:

$$\begin{aligned}
X'_v &= C_X(\alpha) = C_X^0 + C_X^{\alpha_1}\alpha + C_X^{\alpha_2}\alpha^2 + C_X^{\alpha_3}\alpha^3 + C_X^{\alpha_4}\alpha^4,\\
K'_v &= C_K(\beta,\bar{p},\bar{r},\delta_r) = C_K^{\beta}\beta + C_K^{\bar{p}}\bar{p} + C_K^{\bar{r}}\bar{r} + C_K^{\delta_r}\delta_r,\\
Y'_v &= C_Y(\beta,\bar{p},\bar{r},\delta_r) = C_Y^{\beta}\beta + C_Y^{\bar{p}}\bar{p} + C_Y^{\bar{r}}\bar{r} + C_Y^{\delta_r}\delta_r,\\
M'_v &= C_M(\alpha,\bar{q},\delta_e) = C_M^{\alpha}\alpha + C_Z^{\bar{q}}\bar{q} + C_M^{\delta_e}\delta_e,\\
Z'_v &= C_Z(\alpha,\bar{q},\delta_e) = C_Z^{\alpha}\alpha + C_Z^{\bar{q}}\bar{q} + C_Z^{\delta_e}\delta_e,\\
N'_v &= C_N(\beta,\bar{p},\bar{r},\delta_r) = C_N^{\beta}\beta + C_N^{\bar{p}}\bar{p} + C_N^{\bar{r}}\bar{r} + C_N^{\delta_r}\delta_r.
\end{aligned} \tag{6}$$

Inviscid hydrodynamic effects are represented with a generalized added inertia matrix (Fossen, 1994). Due to vehicle symmetry, it can be represented in Equation (7), where the submatrices $\mathbf{M}_f$, $\mathbf{C}_f$, and $\mathbf{J}_f$ represent the added mass, hydrodynamic coupling, and added inertia, respectively. Both viscous and inviscid coefficients are available (Page and Mahmoudian, 2020):

$$\mathbf{M}_f = \begin{pmatrix} \mathbf{M}_f & \mathbf{C}_f^T \\ \mathbf{C}_f & \mathbf{J}_f \end{pmatrix} = -\begin{pmatrix} X_{\dot{u}} & 0 & 0 & 0 & 0 & 0 \\ 0 & Y_{\dot{v}} & 0 & 0 & 0 & Y_{\dot{r}} \\ 0 & 0 & Z_{\dot{w}} & 0 & Z_{\dot{q}} & 0 \\ 0 & 0 & 0 & K_{\dot{p}} & 0 & 0 \\ 0 & 0 & M_{\dot{w}} & 0 & M_{\dot{q}} & 0 \\ 0 & N_{\dot{v}} & 0 & 0 & 0 & N_{\dot{r}} \end{pmatrix}. \tag{7}$$

Forces and moments due to fluid inertia can then be described as in Brennen (1982). These are nondimensionalized by $0.5\rho L^3$, $0.5\rho L^4$, and $0.5\rho L^5$:

$$\begin{bmatrix} \mathbf{f}_i \\ \mathbf{m}_i \end{bmatrix} = -\mathbf{M}_f \begin{bmatrix} \dot{\mathbf{v}}_1 \\ \dot{\mathbf{v}}_2 \end{bmatrix}, \tag{8}$$

$$\begin{aligned}
X'_{\dot{u}} &= \frac{X_{\dot{u}}}{0.5\rho L^3}, \qquad K'_{\dot{p}} = \frac{K_{\dot{p}}}{0.5\rho L^5},\\
Y'_{\dot{v}} &= \frac{Y_{\dot{v}}}{0.5\rho L^3}, \qquad M'_{\dot{q}} = \frac{M_{\dot{q}}}{0.5\rho L^5},\\
Z'_{\dot{w}} &= \frac{Z_{\dot{w}}}{0.5\rho L^3}, \qquad N'_{\dot{r}} = \frac{N_{\dot{r}}}{0.5\rho L^5},\\
Y'_{\dot{r}} = N'_{\dot{v}} &= \frac{Y_{\dot{r}}}{0.5\rho L^4}, \qquad Z'_{\dot{q}} = M'_{\dot{w}} = \frac{Z_{\dot{q}}}{0.5\rho L^4}.
\end{aligned} \tag{9}$$

Total hydrodynamic forces and moments are then calculated by summing both viscous and inviscid terms. Dynamic modeling of the AUV system was completed in a hydrodynamics and multi-body physics co-simulation. Hydrodynamic terms are calculated in Simulink and applied to the multi-body physics simulation in MSC ADAMS, which also makes the 3D visualizations. The simulation is configured to solve at 100 Hz. Computational time is roughly 15 minutes for 2 minutes of simulated time.

Evaluation of the proposed algorithm was initially completed through direct comparison to a standard ILOS control strategy (Fossen and Lekkas, 2017) in simulation. Each control variant was run through three scenarios: no disturbances, mild constant disturbance, and strong, time varying disturbance. All tests start with the vehicle off of the prescribed path similar to a GPS relocalization upon surfacing.

The prescribed path is a Dubins curve from $[x, y, \phi] = [-20, -5, 0]$ to $[30, 50, 0]$ to $[70, 0, \pi]$ with turn radius of $\rho = 20$ m. The initial starting location of the vehicle is $[-20, 0, 0]$ to help evaluate path convergence and controller stability.

The two tested guidance strategies were individually manually tuned to maximize their performance, thus allowing strategy comparison of different control strategies operating in respective optimal configurations. Both strategies utilize a proportional-integral heading tracker with $K_P = 15$,

$K_I = 1$ for the standard ILOS controller and $K_P = 5$, $K_I = 0$ for the proposed strategy. The standard ILOS controller was simulated with an adaptive lookahead of $\alpha = 0.1r$ with $r = \frac{1}{y_e}$, adaptation gain of $\gamma = 4e-3$, and minimum and maximum lookahead distances $\Delta_{min} = 0.5\rho$ and $\Delta_{max} = 1.5\rho$. The relatively long lookahead distances and slow adaptation gains are required to minimize the possibility of oscillations while converging towards the prescribed path. Conversely, the proposed guidance strategy with Dubins replanning was able to be tuned much more aggressively as the replan algorithm ensures that the path following controller will always operate in a region close to a path. This also enables the use of a constant lookahead distance of $\Delta = 0.1\rho$ and relatively fast adaptation gain of $\gamma = 1.5e-2$. For this paper, we consider a constant rendezvous distance of $\delta = 1.3\rho$. Adaptive rendezvous distance will be considered in future work. Additionally, the vehicle is commanded to maintain a constant surge speed of 1 m/s at all times. Adaptive speed control could also be examined to further optimize the system response.

4.2. Simulation Results

Evaluation of the proposed method was first completed in simulation. The results are clustered based on the disturbance applied. Presented is the actual path followed by the controller, the (unsigned) cross-track error, the mean cross-track error, and the standard deviation. In all scenarios, the proposed method detects that the vehicle is far from the prescribed path at the start of the simulation. It then generates a new rendezvous path that will drive the vehicle to converge to the prescribed path.

4.2.1. No Disturbance

The no disturbance scenario is the easiest case for each controller. Figure 7a shows the paths followed. Figure 7b shows the cross-track error of each simulation. The cross-track error can effectively be broken into two separate segments. During the first segment, the vehicle's position converges to the prescribed path. Both the ILOS and proposed guidance strategy converge at a similar rate (Table 2). The second stage is the path tracking portion. This is where the difference between the standard approach and the proposed method is most obvious. Due to the aggressive tuning and smooth Dubins approach, the replan method is capable of tracking the prescribed path after convergence with very little overshoot or oscillation. This is in contrast to the standard ILOS approach which exhibits oscillatory behavior. To an extent, this oscillation can be reduced in the ILOS approach at the cost of convergence rate and disturbance rejection.

4.2.2. Mild Disturbance

With a constant disturbance of 10% of vehicle velocity, the differences in the control strategies becomes more obvious (Figure 8). The disturbance is defined with base components along each axis

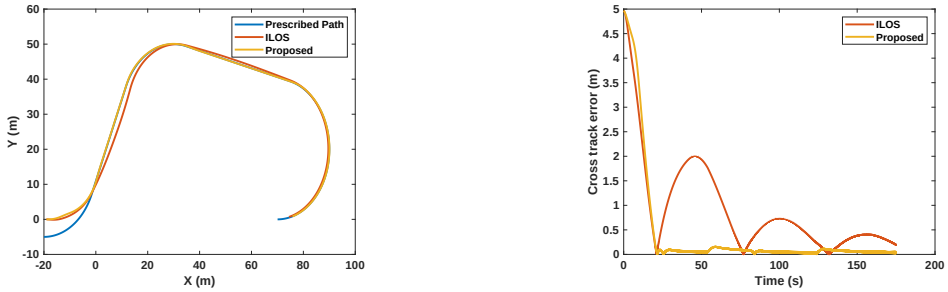

Figure 7. Controller evaluation with no disturbances. (a) 2D paths followed during the test. (b) Unsigned cross-track error. The proposed controller enables the controller to converge towards zero error quickly and effectively eliminates overshoot and oscillation.

Table 2. No disturbance scenario. With zero disturbances applied, the replan scenario enables the AUV to converge at a similar rate to the standard integral line-of-sight control strategy while eliminating overshoot behavior.

Control Strategy	Mean Error	Std Dev	Rise Time (s)
ILOS	0.9295	0.98	21.1
Proposed	0.4069	1.0824	21.6

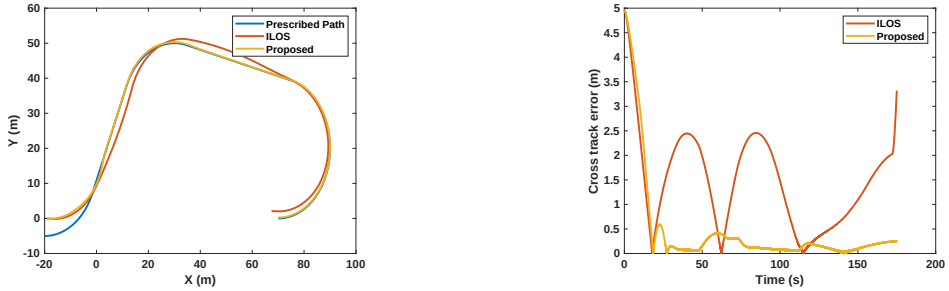

(a) **(b)**

Figure 8. Controller evaluation with mild constant disturbance of $[0.1, 0.1]$ m/s. (a) Paths followed during the test. (b) Unsigned cross-track error. The proposed method enables the path following algorithm to be tuned more aggressively which results in a system more capable of rejecting disturbances.

Table 3. Mild disturbance scenario. With the minor disturbance of 0.1 m/s in X and Y directions, the aggressive tuning of the replan scenario enables it to quickly reject changes in sideslip angle compared to the standard integral line-of-sight controller.

Control Strategy	Mean Error	Std Dev	Rise Time (s)
ILOS	1.4868	0.9690	17.8
Proposed	0.4554	0.9774	18.5

defining the 2D simulated mission environment (Figure 9a). The velocity and direction of the mild disturbance is defined by its principal components in Equation (10) in meters per second:

$$\mathbf{V}_{mild} = [V_x, V_y]^T = [0.1, 0.1]^T. \tag{10}$$

Specifically, the standard ILOS system with its relatively slow adaptation gain is unable to quickly reject the disturbance current when tracking a new straight segment as the sideslip estimate takes time to update. This results in a large mean error of 1.4868 m (Table 3). Conversely, the aggressive tuning of the proposed method is able to quickly adapt to the changing sideslip conditions and track the prescribed path through the entire course.

4.2.3. Strong Disturbance

Large, time varying currents are the most challenging scenario tested for this paper. In this scenario, the disturbance currents applied are shown in Figure 9a. The disturbance is a linear combination of two randomly sampled Gaussian distributions along each principal 2D axis ($\mathbf{V}_{strong} = [V_x, V_y]^T$), each with a mean of 0.15 m/s and update rate of 0.1 Hz. The mean time varying flow velocity in each principle direction (V_x and V_y) was chosen to be representative of open ocean (one degree of latitude away from oceanic currents). Furthermore, while oceanic currents such as the Gulf Stream typical vary on timescales of years to decades (Dong et al., 2019), the rate of 0.1 Hz was selected to challenge the controller(s) considerably more than would be present in the environment.

Between updates, the signal is linearly interpolated to result in a smooth signal. With this challenging scenario, the proposed method is still able to accurately track the prescribed path

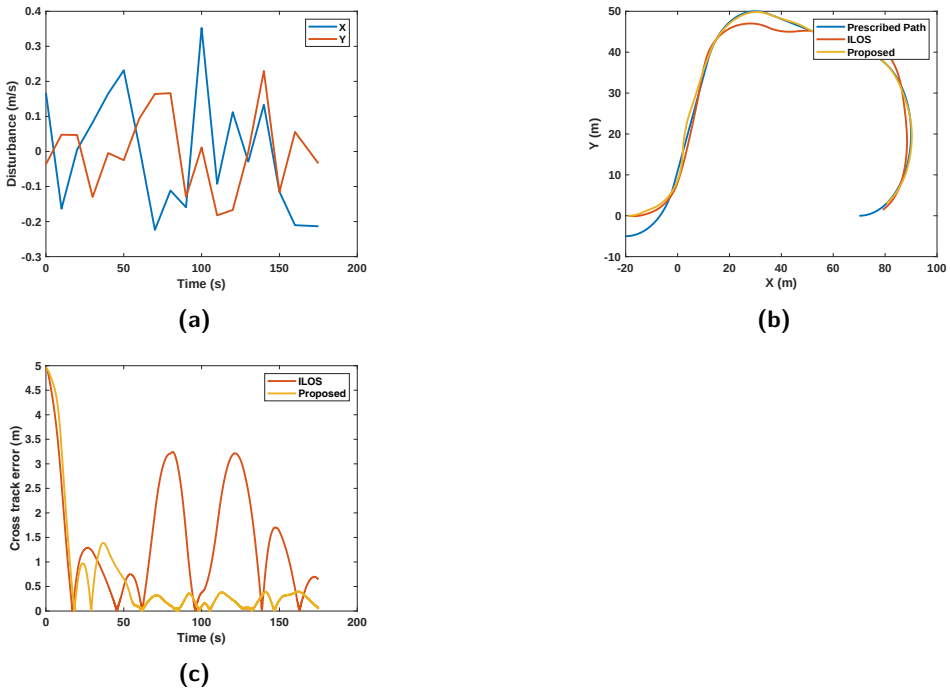

Figure 9. Strong disturbance scenario. (a) The time varying disturbance applied to the vehicle. The disturbance is a randomly sampled Gaussian distribution with 0.1 Hz update and linear interpolation between updates. (b) Paths followed during the test. (c) Unsigned cross-track error. The proposed method is much better at tracking in challenging scenarios.

Table 4. Strong disturbance scenario. With heavy time varying disturbances the control strategy with replan is able to rapidly adapt to changing conditions.

Control Strategy	Mean Error (m)	Std Dev (m)	Rise Time (s)
ILOS	1.4762	1.1564	17.1
Proposed	0.6397	1.0495	18.2

throughout the test while the standard ILOS system has some trouble adapting to the changing sideslip conditions, Figure 9b. This is reflected in the unsigned cross-track error where the standard ILOS system deviates larger than 2 m away from the path multiple times (Figure 9c). Overall the proposed algorithm is capable of tracking this path with a mean error of 0.6397 m compared to that of the standard ILOS, 1.4762 m (Table 4).

Through all the tested scenarios, we have demonstrated that the ability to combine path planning with efficient path tracking enables more accurate path following in challenging scenarios than a path tracker alone. The enabling idea behind this is that if the cross-track watchdog ever detects that the vehicle is far away from the prescribed path, such as a GPS update, it will augment that path with a rendezvous path based on Dubins curves. As the vehicle is never far from the augmented path, the following algorithm can be tuned to aggressively track the path. This aggressive path following tune enables the vehicle to accurately track the augmented path through strong, time varying currents and through changes in curvature. Without the augmented rendezvous path, the aggressive path following algorithm would be unable to accurately track the path. To confirm this, the strong current scenario was tested with two additional control tunes, one with aggressive path following like the proposed algorithm and one with relaxed path following parameters. All three tested control tunes are shown in Figure 10. In the relaxed scenario, the vehicle is unable to react quickly to changing sideslip conditions caused by the disturbance. In the aggressive scenario, the ILOS system causes

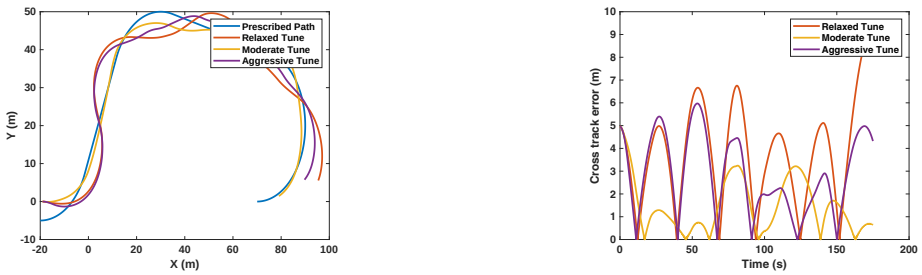

(a) (b)

Figure 10. Evaluating the integral line-of-sight controller in the strong current scenario with two additional controller tunes. A more relaxed tune is unable to compensate for the changing currents fast enough and fails to accurately track the path. A more aggressive tune causes strong oscillations and overshoots. (a) Paths followed with the various ILOS controller tunes and (b) unsigned cross-track error.

(a) (b)

Figure 11. (a) The Purdue University custom ASV is a catamaran platform with dual thrusters providing differential steering ability. It is a low-cost platform capable of algorithm validation. (b) Oceanserver Iver3 AUV used for field trials. The Iver3 is a commercially available platform that operates in a frontseat-backseat manner.

overshoot and oscillation as it tries to converge to the path quickly. The moderate control tune attempts to balance between these two extremes, but is unable to track the path as well as the proposed guidance strategy.

5. Field Experiments

5.1. Field Experimental Setup

Following initial evaluation in the simulation, the control algorithm was translated into Python and implemented onboard a custom ASV and Oceanserver Iver3 AUV (Figures 11a and 11b, respectively). Both vehicles operate on what is referred to as a frontseat-backseat paradigm. In this setup, a frontseat controller (manufacturer provided for commercial vehicles like the Iver3) maintains low-level operation of the vehicle such as maintaining desired depth, heading, and speed through disturbances. The frontseat controller also fuses all sensor information into a localization estimate. The backseat controller is user specified and is capable of providing commands and taking over control from the frontseat through a frontseat-backseat communications link. Testing for both vehicles was trialed in the Fairfield Lakes pond near Purdue University. The pond is approximately 7–8 m deep, 600 m long, and 150 m wide.

The specific implementation of the controller was completed using the Robotic Operating System (ROS) onboard the backseat computer of each vehicle. The controller operates on multiple layers. The path planning layer interprets a set of waypoints and headings from the offboard mission planner to generate a prescribed path to be followed based on Dubins curves. The Dubins path rendezvous

planning then compares the current location to the prescribed (or previously augmented path) and decides if a new rendezvous path is required based on cross-track error. If the cross-track error is larger than 2 m a new path is drawn to drive the Iver3 back towards the prescribed path at a location 25 m ahead on the prescribed path. If the cross-track error is less than the threshold, the Iver3 continues operating on the prescribed path or previously augmented path. The path following layer is a standard implementation of the integral line-of-sight algorithm with a fixed lookahead distance of 6 m and a nominally zero adaptation gain due to the lack of currents in the pond environment. At the path tracking layer, the calculated heading, speed, and depth are transmitted to the frontseat for interpretation and action onboard the frontseat computer. The entire backseat control loop operates at 1 Hz.

The control algorithm was first implemented on Purdue University's custom ASV BREAM (Boat for Robotic Engineering and Applied Machine-Learning) (Lambert et al., 2021) (Figure 11a). This was done to verify control algorithm functionality in the real world with minimal risk to equipment. The ASV is a low-cost and modular catamaran platform with dual thrusters set up in a differential steering configuration (Figure 11a). All components onboard the ASV are low cost and commercially available off the shelf. Items were purchased primarily from online retailers and led to a total unit cost under US$1800 when not including mission-specific additions for sensing and endurance capabilities. A detailed description of the vehicle can be found in Lambert et al. (2020).

The frontseat controller on the ASV performs basic vehicle control such as vehicle speed and heading control using PID controllers while the backseat controller performs higher-level control decisions. Both systems are networked and utilize the ROS to standardize communications and messaging. Specifically, the frontseat computer reads sensor values and transmits a fused position and orientation to the backseat. The backseat then computes a desired heading and velocity with respect to the active path and transmits that back to the frontseat computer. The frontseat then takes those values and computes motor outputs for the differential steering system.

The ASV is capable of operating with a significantly reduced sensing and computational capability compared to an equivalently capable AUV. This is due to the consistent ability to receive high accuracy and frequency location updates from GNSS systems. As the proposed method is primarily meant as a long-range navigational solution the ASV was able to be deployed with only a GPS and compass for sensing capability, and did not need to perceive its surrounding environment.

Testing consisted of performing a continuous circuit comprised of six waypoints (one repeated) linked with a Dubins curve (Figure 12). Tuning of the controllers was completed in three phases. First, the reference tracking controller on the frontseat was tuned to be able to accurately and aggressively track a heading with minimal overshoot through disturbances. Then the ILOS controller

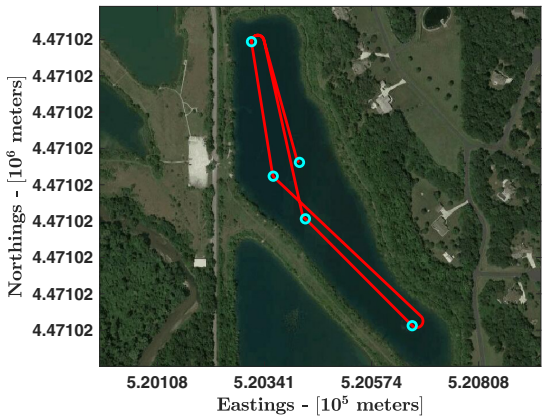

Figure 12. Prescribed path to be followed by the ASV during operation in Fairfield Lakes. The six waypoints given to the mission controller from the offboard mission planner are shown in blue. The northernmost waypoint was provided twice to create a closed curve.

was tuned to track a fixed Dubins curve with reasonable accuracy. Finally, the replan method was implemented and tuned to efficiently rendezvous with the prescribed path following large disturbances. As the simulations discussed in Section 4.2 were designed for rudder-based AUV locomotion the replan variables were tuned from scratch and were not representative of those used in the simulation.

In addition to functionality implementation and testing on an ASV the control algorithm was fully tested on the Oceanserver Iver3 AUV. As both the ASV and Oceanserver Iver3 backseats utilized ROS, Python, and a frontseat-backseat control strategy a nearly identical controller was run on both vehicles. To facilitate frontseat-backseat in situ communication on the Iver3, a custom communications package was created to interface with the frontseat over NMEA messaging. The major differences between the ASV and AUV implementations were data acquisition protocols on the backseat for receiving the vehicle state from the frontseat (NMEA vs TCP/IP), tunable controller parameters for lookahead distance (Δ), rendezvous distance (δ), adaptation gain (γ), and forcing the initial replan towards the prescribed path to route the vehicle to the beginning of the path.

For Iver3 AUV testing, two paths were repeated for a total of 30 hours and 100 km of operation. To evaluate replanning convergence the Iver3 local compass calibration was not completed. This accelerated the localization estimate degradation rate while submerged. Additionally, the AUV was commanded to surface at regular intervals by cycling between being surfaced for 45 s and submerged for 120 s. The combination of compass miscalibration and surfacing/submerged operations triggered the controller to generate rendezvous paths on the majority of surfacing events.

The controller implemented onboard the Iver3 backseat was identical in function to the one implemented in the simulation. The Iver3 frontseat has a full guidance, navigation, and control system with state estimation and localization smoothing that is used for providing low-level control of the vehicle. The controller was experimentally tuned based on initial values from the simulation. Due to the frontseat-backseat setup, only parameters associated with the ILOS path following and Dubins path rendezvous planner were adjustable while reference tracking layer was set by the manufacturer. The proposed strategy had the following parameters: lookahead distance $\Delta = 0.6\rho$, rendezvous distance $\delta = 2.5\rho$, and adaptation gain $\gamma = 0$. The relatively longer rendezvous distance experimentally was necessary to prevent the injection of unnecessary circle maneuvers as shown in Figure 13a. Adaption gain was set to zero during pond testing due to the lack of any appreciable steady state disturbance current.

Tuning of the rendezvous distance (δ) is critical for mission efficiency. If the rendezvous distance is set too short it will result in injected circle maneuvers occasionally on surfacing. In Figure 13a the AUV surfaced along a straight segment of path slightly off course. The short rendezvous distance caused the Dubins path to be recalculated to include a full circle maneuver versus approaching the initial plan further ahead on the path using a less disruptive path. If the rendezvous distance is set too long then the replan may cut off critical portions of the overall path to create a shorter path. In Figure 13b the prescribed path follows a linear approach into a waypoint at the top left of the

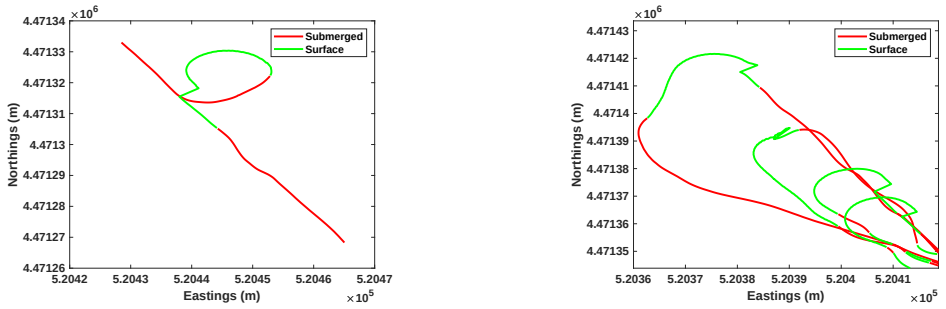

Figure 13. Tuning the rendezvous distance. (a) When the rendezvous distance is too short extra circles can be injected. (b) When the rendezvous is too long the prescribed path may not be followed through corners.

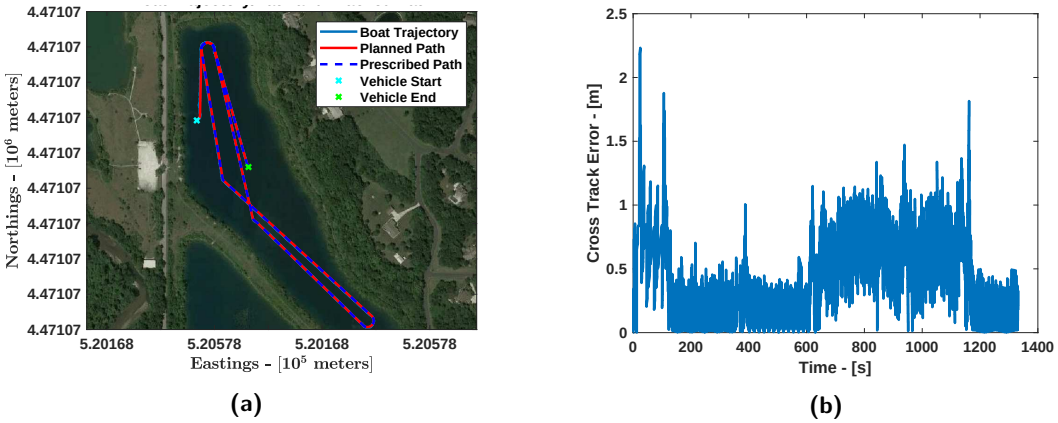

Figure 14. Path testing of the ASV. In this test the prescribed path consists of a set of six waypoints connected through Dubins curves. (a) The boat trajectory, prescribed path, start, and end points. (b) The vehicle cross-track error to the prescribed path. Due to the continuous localization of the boat, replans were not needed during operation as no discontinuities in positioning were encountered.

frame before returning towards the bottom right along the southerly path. Due to a long rendezvous distance on most occasions the AUV will not follow the prescribed path but will instead plan an overall shorter path that fails to meet the mission objectives. In the future, an adaptive rendezvous distance will be considered to promote overall efficiency and path completion.

5.2. Field Experimental Results

ASV surface testing of the proposed control algorithm was done in such a way that the vehicle would complete the prescribed path, finish its given mission, and then stop and await further instructions. Thus the tests were distance rather than time based with the vehicle controllers inactive after path completion; therefore, each trajectory shown is a separate vehicle deployment. This can be seen in Figure 14a with the vehicle drifting after prescribed path completion.

The vehicle performed laps of the mission shown in the Figure 12 pattern over several days of testing with a variety of disturbance conditions (primarily wind). Three individual sessions, each 1 hour long, were conducted to tune the parameters of the controller to the ASV specifically and tune the PID gains to be as aggressive as possible without creating vehicle oscillation about the prescribed path. The resulting parameters used for the testing were $\rho = 10$, lookahead distance $\Delta = 0.4\rho$, rendezvous distance $\delta = 2\rho$, and adaptation gain $\gamma = 0$.

After tuning of controller parameters was complete, the vehicle was deployed over the course of approximately 2 hours (four asynchronous deployments) and 8 km of testing. Across all four deployments the overall average cross-track error was 0.21 m and on average only an initial replan to converge with the path from the vehicle's starting position was needed. This was largely due the vehicle's ability to rapidly gather accurate localization feedback data and enact actuator commands at 10 Hz.

Despite the disturbances present in the environment the replan method was not required during the vast majority of operation. This is due to the high accuracy and frequency feedback capabilities afforded by operation on the surface with a GNSS receiver. Figure 14 shows the trajectory and cross track followed during a single deployment. The cross-track error never exceeded 2.23 during the asynchronous test; thus a replan was never initiated. Figure 15 shows the trajectory followed during another deployment with a focus on the initial replan.

To test the limits of the path following controller's ability to follow the prescribed path the vehicle was also deployed with attached devices to alter the dynamics of the vehicle such as a mobile docking station and an acoustic beacon. Even with these additions, the controller was able to easily follow the prescribed path without any changes to the low-level vehicle actuation controller. This shows

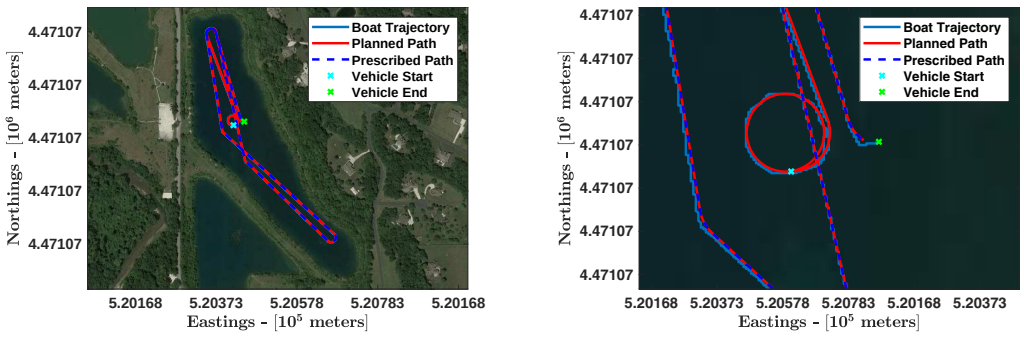

Figure 15. (a) Deployment of the ASV on the six-point path resulted in consistent operation over the entire course. However, (b) differences in the approach phase were encountered depending on the starting point and orientation of the ASV.

that when operating with high accuracy and frequency ground-truth localization information, such as that present from GNSS systems on the surface, the replan ability of the proposed method becomes less relevant. This is shown in Figure 15a as the path is approximately the same as if no replan methodology was implemented. Thus the trajectory of the vehicle represents that of methods without a replan ability; however, the method still achieves low-error paths matching that of typical methods with minimal additional computational load.

To show the need for the proposed method when high frequency and accuracy localization is not present, experimental testing of the method on the AUV was completed using two distinct patterns in Fairfield Lakes park near Lafayette, Indiana, USA. For the presented results, the Iver3 was deployed in a frontseat-backseat configuration using the Iver3 servo commands to overwrite the vehicle navigation system. Servo commands were issued approximately at 1 Hz with depth set to alternate between 2 m and surfaced at regular intervals for GPS localization updates. Vehicle surge speed was commanded at a constant 2 knots. In the presented results the vehicle proceeded around the prescribed path in a counterclockwise direction. A total of 30 hours of operation was completed, 17 hours of operation on a long pattern divided into three separate runs, one of 9 hours, a second one of 4 hours, both of them with the Dubins path rendezvous planner enabled, and a third one of 4 hours with the Dubins path rendezvous planner disabled, additionally 5 hours on a shorter pattern, and 8 hours tuning the controller parameters. Presented here are the results from the two 4-hour runs on the long pattern for overall performance, and the 5 hours of the short pattern straight line convergence test.

Figures 16a and 16b show 8 hours of testing overlaid. In these plots, the green portions of the trajectory located at a depth of less than 0.5 m are referred to as surfaced, while that deeper than 0.5 m is submerged. Of note in the overall results is that, despite tuning efforts, the system still injected circle maneuvers very rarely upon resurfacing. This effect could not be entirely tuned out without having a negative impact on cornering performance. Due to the relocalization problem the system performed a replan approximately every 3 minutes.

Figures 16c–16f show a single lap of the prescribed path and associated cross-track error with and without the Dubins path rendezvous planner. In the single lap it is clearer that the proposed method is capable of rapidly driving convergence towards the prescribed path without significant overshoot. The cross-track error in this lap had a mean of 1.14 m, while over the entire test the mean was 1.32 m due to the short-lived large cross-track error during the injected circle maneuvers. Of more importance than the average cross-track error is how quickly the system is able to return to the prescribed path after a GPS relocalization. In the presented single lap the system surfaced three times. One of those surfacings had a cross-track error of more than 3 m. These relatively large deviations triggered replans that drove the vehicle to converge to the prescribed path with minimal overshoot as indicated in the simulation results.

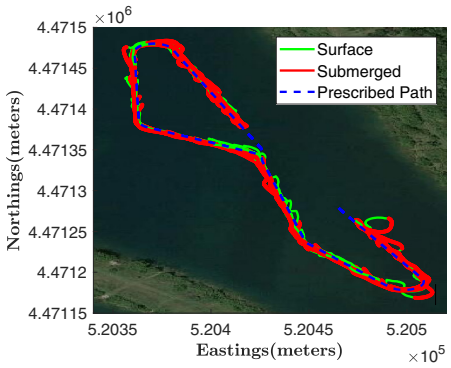

(a) Replan on.

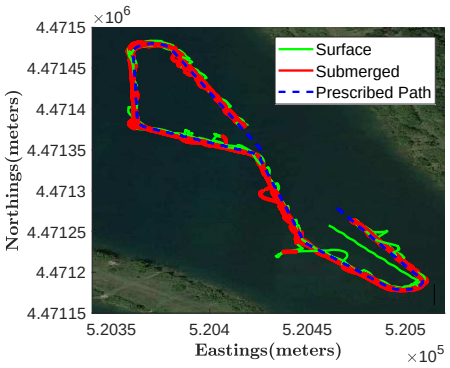

(b) Replan off.

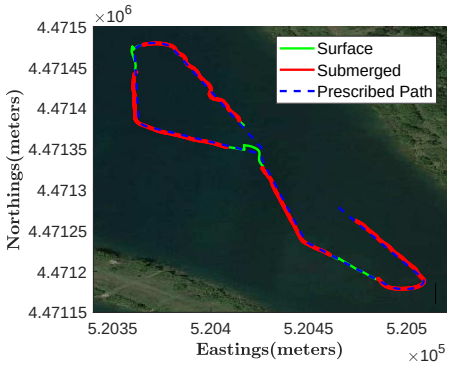

(c) Replan on.

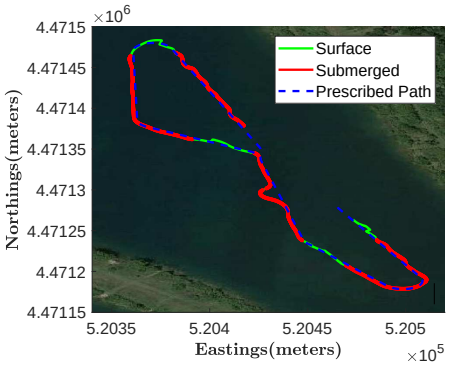

(d) Replan off.

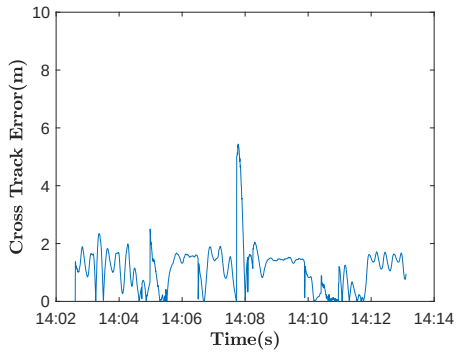

(e) Replan on.

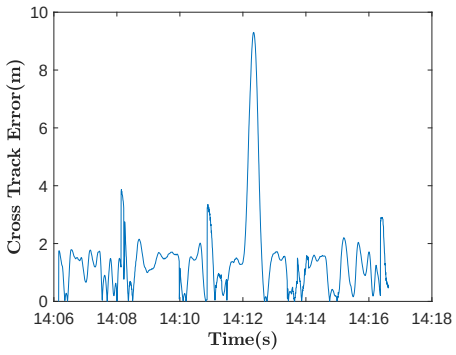

(f) Replan off.

Figure 16. Extended duration testing of the proposed planner/follower architecture on an Oceanserver Iver3. (a) The overall trajectory on 4 hours (15 km) of testing with the Dubins path rendezvous planner on. (b) The overall trajectory on 4 hours (15 km) of testing with the Dubins path rendezvous planner off. (c) A single lap of of the trajectory with the Dubins path rendezvous planner on. (d) A single lap of of the trajectory with the Dubins path rendezvous planner off. (e) The cross-track error from the original prescribed path during the single lap with the Dubins path rendezvous planner on. (f) The cross-track error from the original prescribed path during the single lap with the Dubins path rendezvous planner off. During the test using the Dubins path rendezvous planner the mean absolute cross-track error was about 1.14 m with a standard deviation of 0.74 m. In the the scenario with the Dubins path rendezvous planner off the mean of the absolute cross-track error was about 1.41 m with a standard deviation of 1.38 m.

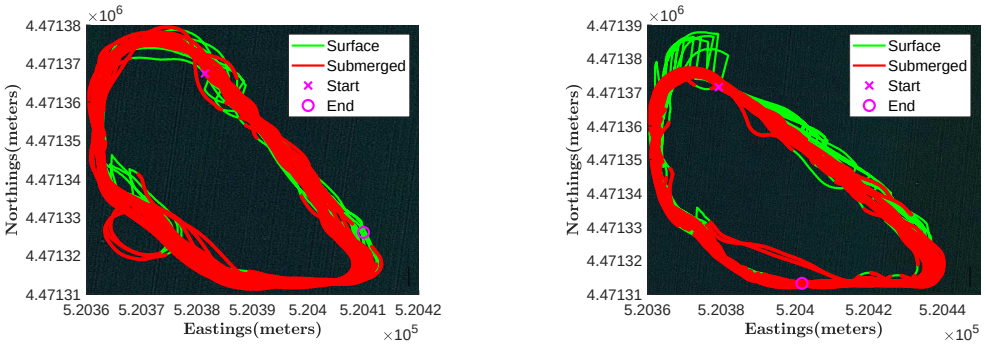

Figure 17. Short path testing of the AUV. In these tests, the prescribed path consisted of waypoints representing a tri-oval with its major axis aligned northwest to southeast. These tests evaluated the ability of the AUV to converge to a straight line segment as needed for operation such as side scan sonar and docking. (a) 20-m linear segment and (b) 40-m linear segment.

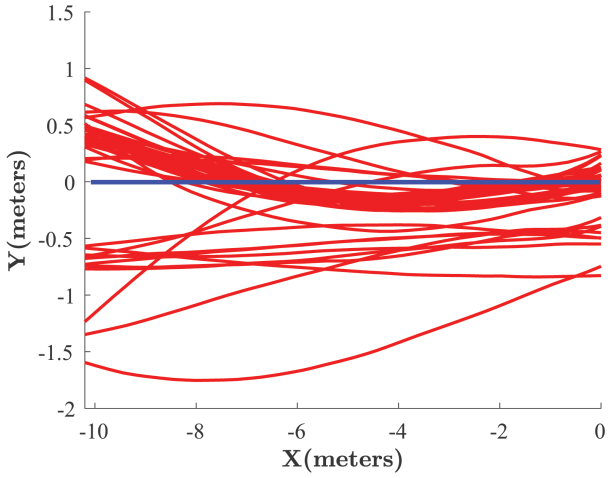

Figure 18. The proposed method is capable of converging to a linear path as required for real-world sonar survey or docking operations. Shown is a segment of recorded position data from Iver3 testing showing repeatable convergence of within ± 1 m of the prescribed path (blue).

As an additional trial, the proposed method was tested on two shorter paths featuring a roughly triangular maneuver pattern along with a disconnected straight line segment as would exist during either side scan survey or docking operations. This operational testing required the AUV to replan at least twice per lap at both the start and end of the straight line path. Two different straight length segments were trialed, a 20-m segment (Figure 17a) and a 40-m segment (Figure 17b). Total testing time was approximately 5 hours and 17 km of distance.

Of critical importance to testing in the real world is the ability to track straight line paths accurately. If we consider the straight line segment we can see that the system is capable of converging to the path and tracking it with high accuracy over a large number of attempts (Figure 18). In fact, all trials are within 1 m of cross-track error by the end of the 20-m linear pattern.

As can be seen in Figures 19b and 19a, when operating on the surface the Iver3 performs similarly to the ASV, does not require replans, and follows the prescribed path nearly identically to the initially established mission. However, when commanded to alternate between 0 and 2 m of depth, the localization estimate degrades over time. This results in abrupt cross-track errors to appear

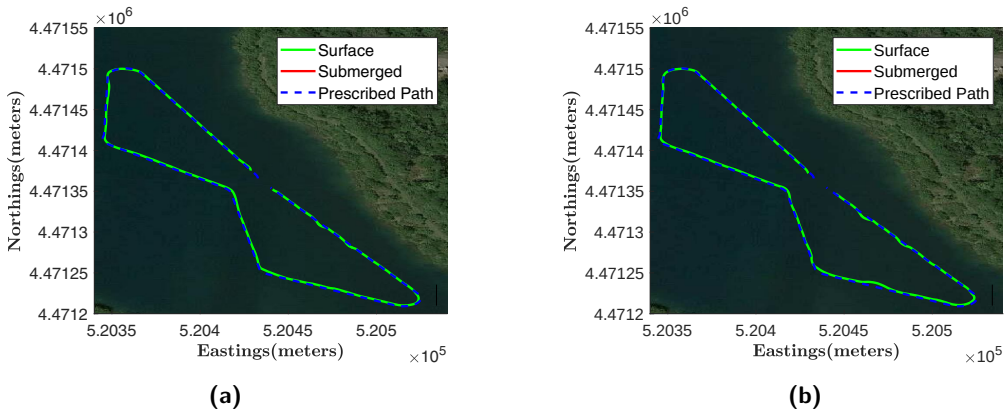

Figure 19. (a) Deployment of Iver3 AUV on a seven-point surface mission with Dubins path rendezvous planner enabled shows a similar performance when compared to (b) a deployment of Iver3 on the same seven-point surface mission with the Dubins path rendezvous planner disabled.

upon surfacing and receiving GNSS localization information (Figures 16a and 16b). These abrupt cross-track error changes are where the strengths of the proposed control algorithm are easier to identify (Figures 16c and 16d). In these figures, it is possible to observe how the Dubins path rendezvous planner creates a Dubins path to drive the vehicle back towards the prescribed path. The mean absolute cross-track error with the rendezvous Dubins path rendezvous planner enabled is 1.14 m, which is a 23% improvement on the mean absolute cross-track error with planner disabled, which exhibits an error of 1.38 m. This demonstrates the value of the proposed methodology over current methods when encountering inconsistent localization during the mission such as is common in underwater vehicle operations.

Through 30 hours of experimental underwater testing, we have demonstrated the algorithm's ability to perform in the real world with commercially available systems such as the Oceanserver Iver3. Over the entire test, the proposed method resulted in a cross-track error of less than 2 m 82% of the time and was able to rapidly adapt to intermittent updates in location due to GPS surfacing as shown in Figure 16e. Additionally, the proposed method showed great potential to be deployed on real-world missions such as collecting sonar data or performing underwater docking due the rapid convergence to less than 1 m cross-track error when operating on straight line segments.

6. Conclusion

Presented in this work was the vehicle-level guidance strategy that efficiently links a high-level mission strategy to actionable control signals for the vehicle to follow. The proposed method was evaluated in simulation against comparable recent controller designs and then extensively trialed across domains in the field. Results indicate that the method more accurately tracks prescribed paths through strong disturbances and localization discontinuities.

More specifically, this paper presented a way to combine the classical Dubins path planner with integral line-of-sight control to create an efficient and effective guidance strategy for marine vehicles experiencing strong disturbances and discontinuities in localization estimates. The proposed method adds a Dubins path rendezvous planner at the path planning layer. The Dubins path rendezvous planner injects rendezvous Dubins curves into the prescribed path whenever a sufficiently large cross-track error is detected. The augmented path is then followed using a traditional integral line-of-sight controller. This combined strategy enables the path follower to be tuned to track the path with greater disturbance rejection and faster convergence than would otherwise be feasible. Evaluation of this method has been completed in three systems. First, the method was evaluated against pure integral line-of-sight control in simulation with a variety of scenarios. Then the method

was experimentally tested for 30 hours of operation using an Oceanserver Iver3 AUV. To evaluate cross-domain capability, the method was then implemented onto a custom ASV for 5 hours of operation.

Overall, these field and simulation trials show that the proposed method is efficient, effective, and capable of operating on a range of platforms and domains. Future work with this method is extensive and focuses on expanding from generic mission profiles to specific scientific and research missions. The primary goal in the near term is to apply the proposed method to autonomous docking operations that enable long-term deployments where localization discontinuities are common. The ability to converge to any straight line segment from the prescribed path enables the AUV to automatically plot and track a path towards a docking station located at an arbitrary position and orientation. This is critical for the mobile underwater docking problem as both the AUV and ASV (with attached docking station) need to be able to rendezvous and dock at arbitrary points in the mission as defined by the overall mission planner. In this problem, the ASV needs to navigate towards and along a straight line path at a slow speed during the docking maneuver. The AUV needs to approach the docking station in a straight line path projected from the dock. Once within range, AUV control is handed off to a higher resolution, higher update rate navigation solution for terminal homing. The presented approach will enable field deployment of long-term, persistent fleets for autonomous underwater and surface survey operations when combined with an intelligent multi-vehicle mission planner and adaptable docking system.

Acknowledgments

This material is based upon work supported by NSF 1921060 and ONR N00014-20-1-2085.

ORCID

Brian R. Page https://orcid.org/0000-0002-3634-8944
Reeve Lambert https://orcid.org/0000-0002-0259-2826
Jalil Chavez-Galaviz https://orcid.org/0000-0003-2032-2296
Nina Mahmoudian https://orcid.org/0000-0002-3285-8234

References

Battistelli, G., Hespanha, J., and Tesi, P. (2012). Supervisory control of switched nonlinear systems. *International Journal of Adaptive Control and Signal Processing*, 26(8):723–738.

Battistelli, G., Hespanha, J. P., Mosca, E., and Tesi, P. (2013). Model-free adaptive switching control of time-varying plants. *IEEE Transactions on Automatic Control*, 58(5):1208–1220.

Boissonnat, J.-D., Cérézo, A., and Leblond, J. (1994). Shortest paths of bounded curvature in the plane. *Journal of Intelligent & Robotic Systems*, 11(1–2):5–20.

Borhaug, E., Pavlov, A., and Pettersen, K. Y. (2008). Integral los control for path following of underactuated marine surface vessels in the presence of constant ocean currents. In *2008 47th IEEE Conference on Decision and Control*, pages 4984–4991.

Brennen, C. (1982). A review of added mass and fluid inertial forces. Technical report, Naval Civil Engineering Laboratory.

Bychkov, I., Davydov, A., Kenzin, M., Maksimkin, N., Nagul, N., and Ul'yanov, S. (2019). Hierarchical control system design problems for multiple autonomous underwater vehicles. In *2019 International Siberian Conference on Control and Communications (SIBCON)*, pages 1–6.

Caharija, W., Pettersen, K. Y., Gravdahl, J. T., and Børhaug, E. (2012). Path following of underactuated autonomous underwater vehicles in the presence of ocean currents. In *2012 51st IEEE Conference on Decision and Control (CDC)*, pages 528–535.

Caharija, W., Pettersen, K. Y., Bibuli, M., Calado, P., Zereik, E., Braga, J., Gravdahl, J. T., Sørensen, A. J., Milovanović, M., and Bruzzone, G. (2016). Integral line-of-sight guidance and control of underactuated marine vehicles: Theory, simulations, and experiments. *IEEE Transactions on Control Systems Technology*, 24(5):1623–1642.

Carreras, M., Hernández, J. D., Vidal, E., Palomeras, N., Ribas, D., and Ridao, P. (2018). Sparus II AUV—a hovering vehicle for seabed inspection. *IEEE Journal of Oceanic Engineering*, 43(2):344–355.

Coulter, R. C. (1992). Implementation of the pure pursuit path tracking algorithm. Technical report, The Robotics Institute, Carnegie-Mellon University, Pittsburgh, PA.

Dong, S., Baringer, M. O., and Goni, G. J. (2019). Slow down of the Gulf Stream during 1993–2016. *Scientific Reports*, 9(1).

Dubins, L. E. (1957). On curves of minimal length with a constraint on average curvature, and with prescribed initial and terminal positions and tangents. *American Journal of Mathematics*, 79(3): 497–516.

Fossen, T. I. (1994). *Guidance and Control of Ocean Vehicles*. John Wiley & Sons Inc.

Fossen, T. I. and Lekkas, A. M. (2017). Direct and indirect adaptive integral line-of-sight path-following controllers for marine craft exposed to ocean currents. *International Journal of Adaptive Control and Signal Processing*, 31(4):445–463.

Fossen, T. I., Pettersen, K. Y., and Galeazzi, R. (2015). Line-of-sight path following for Dubins paths with adaptive sideslip compensation of drift forces. *IEEE Transactions on Control Systems Technology*, 23(2):820–827.

Kim, B. S., Calise, A. J., and Sattigeri, R. J. (2007). Adaptive, integrated guidance and control design for line-of-sight-based formation flight. *Journal of Guidance, Control, and Dynamics*, 30(5):1386–1399.

Lambert, R., Li, J., Wu, L.-F., and Mahmoudian, N. (2021). Robust ASV navigation through ground to water cross-domain deep reinforcement learning. *Frontiers in Robotics and AI*, page 289.

Lambert, R., Page, B., Chavez, J., and Mahmoudian, N. (2020). A low-cost autonomous surface vehicle for multi-vehicle operations. In *Global Oceans 2020*, pages 1–5.

Leonard, J. J. and Bahr, A. (2016). *Autonomous Underwater Vehicle Navigation*, pages 341–358. Springer International Publishing, Cham.

Li, B., Moridian, B., Kamal, A., Patankar, S., and Mahmoudian, N. (2018). Multi-robot mission planning with static energy replenishment. *Journal of Intelligent & Robotic Systems*, 95(2):745–759.

Li, B., Page, B. R., Hoffman, J., Moridian, B., and Mahmoudian, N. (2019). Rendezvous planning for multiple AUVs with mobile charging stations in dynamic currents. *IEEE Robotics and Automation Letters*, 4(2):1653–1660.

Mahmoudian, N., Geisbert, J., and Woolsey, C. (2010). Approximate analytical turning conditions for underwater gliders: Implications for motion control and path planning. *IEEE Journal of Oceanic Engineering*, 35(1):131–143.

Manyam, S. G. and Rathinam, S. (2018). On tightly bounding the Dubins traveling salesman's optimum. *Journal of Dynamic Systems, Measurement, and Control*, 140(7).

Nelson, R. C. (1998). *Flight Stability and Automatic Control*, volume 2. WCB/McGraw-Hill, New York.

Oh, S.-R. and Sun, J. (2010). Path following of underactuated marine surface vessels using line-of-sight based model predictive control. *Ocean Engineering*, 37(2):289–295.

Page, B. R. and Mahmoudian, N. (2019). AUV docking and recovery with USV: An experimental study. In *OCEANS 2019 - Marseille*, pages 1–5.

Page, B. R. and Mahmoudian, N. (2020). Simulation-driven optimization of underwater docking station design. *IEEE Journal of Oceanic Engineering*, 45(2):404–413.

Page, B. R., Lambert, R., Galaviz, J. C., and Mahmoudian, N. (2021). Underwater docking approach and homing to enable persistent operation. *Frontiers in Robotics and AI*, volume 8, page 621755.

Pamadi, B. N. (2004). *Performance, Stability, Dynamics, and Control of Airplanes*. AIAA.

Reeds, J. and Shepp, L. (1990). Optimal paths for a car that goes both forwards and backwards. *Pacific Journal of Mathematics*, 145(2):367–393.

Ridao, P., Yuh, J., Batlle, J., and Sugihara, K. (2000). On AUV control architecture. In *Proceedings of the 2000 IEEE/RSJ International Conference on Intelligent Robots and Systems (IROS 2000) (Cat. No. 00CH37113)*, volume 2, pages 855–860.

Rypkema, N. R., Fischell, E. M., and Schmidt, H. (2017). One-way travel-time inverted ultra-short baseline localization for low-cost autonomous underwater vehicles. In *2017 IEEE International Conference on Robotics and Automation (ICRA)*, pages 4920–4926.

Shkel, A. M. and Lumelsky, V. (2001). Classification of the Dubins set. *Robotics and Autonomous Systems*, 34(4):179–202.

Techy, L. and Woolsey, C. A. (2009). Minimum-time path planning for unmanned aerial vehicles in steady uniform winds. *Journal of Guidance, Control, and Dynamics*, 32(6):1736–1746.

Techy, L., Woolsey, C. A., and Morgansen, K. A. (2010). Planar path planning for flight vehicles in wind with turn rate and acceleration bounds. In *2010 IEEE International Conference on Robotics and Automation*, pages 3240–3245.

Tinka, A., Diemer, S., Madureira, L., Marques, E. B., de Sousa, J. B., Martins, R., Pinto, J., da Silva, J. E., Sousa, A., Saint-Pierre, P., and Bayen, A. M. (2009). Viability-based computation of spatially constrained minimum time trajectories for an autonomous underwater vehicle: Implementation and experiments. In *2009 American Control Conference*, pages 3603–3610.

Torrico, C. R., Leal, A. B., and Watanabe, A. T. (2016). Modeling and supervisory control of mobile robots: A case of a sumo robot. *IFAC-PapersOnLine*, 49(32):240–245.

Viswanathan, V. K., Lobo, Z., Lupanow, J., von Fock, S. S., Wood, Z., Gambin, T., and Clark, C. (2017). AUV motion-planning for photogrammetric reconstruction of marine archaeological sites. In *2017 IEEE International Conference on Robotics and Automation (ICRA)*, pages 5096–5103.

Xu, H., Zhang, Y., and Feng, X. (2004). Discrete hierarchical supervisory control for autonomous underwater vehicle. In *Proceedings of the 2004 International Symposium on Underwater Technology (IEEE Cat. No. 04EX869)*, pages 417–421. IEEE.

Zhang, T., Li, D., and Yang, C. (2017). Study on impact process of AUV underwater docking with a cone-shaped dock. *Ocean Engineering*, 130:176–187.

Zhou, M., Bachmayer, R., and deYoung, B. (2019). Mapping the underside of an iceberg with a modified underwater glider. *Journal of Field Robotics*, 36(6):1102–1117.

How to cite this article: Page, B. R., Lambert, R., Chavez-Galaviz, J., & Mahmoudian, N. (2022). Path following using rendezvous Dubins curves and integral line-of-sight for unmanned marine systems. *Field Robotics, 2,* 1920–1942.